

RESEARCH ARTICLE OPEN ACCESS

Gypsum Binder With Increased Water Resistance Derived From Membrane Water Desalination Waste

Valentin Romanovski¹  | Dmitry Moskovskikh^{2,3} | Hongbin Tan⁴ | Kirill Kuskov² | Sergey Volodko³ | Abayomi Adewale Akinwande⁵ | Rajiv Periakaruppan⁶ | Fanyue Kong¹ | Xiaoling Ma⁴ | Feihua Yang⁷ | Maksim Kamarou⁸

¹Department of Materials Science and Engineering, University of Virginia, Charlottesville, Virginia, USA | ²Science and Research Centre of Functional Nano-Ceramics, National University of Science and Technology "MISIS", Moscow, Russia | ³Moscow Polytechnic University, Moscow, Russia | ⁴School of Materials and Chemistry, Southwest University of Science and Technology, Mianyang, China | ⁵Department of Metallurgical and Materials Engineering, Federal University of Technology, Akure, Ondo State, Nigeria | ⁶Department of Biotechnology, PSG College of Arts & Science, Coimbatore, Tamil Nadu, India | ⁷State Key Laboratory of Solid Waste Resource Utilization and Energy Saving Building Materials, Beijing, China | ⁸International Information and Analytical Center for Technology Transfer, Belarusian State Technological University, Minsk, Belarus

Correspondence: Valentin Romanovski (rvd9ar@virginia.edu)

Received: 4 July 2024 | **Revised:** 26 September 2024 | **Accepted:** 1 October 2024

Funding: The study was carried out with the financial support of the Moscow Polytechnic University within the framework of the Kapitsa grant program.

Keywords: additive | plaster binder | production waste | strength | synthetic gypsum | waste recycling | water resistance | water resistance coefficient

ABSTRACT

A method has been developed for separating a mixture of calcium, magnesium and sodium sulfates obtained through the interaction of sulfuric acid and waste from the water purification process generated by using membrane filters. The primary goal of this method is to extract gypsum and produce gypsum-based binders. Patterns were identified regarding how various types, ratio and quantities of additives: blast furnace slag, granite screenings, portland cement, electric steel smelting slag affect the water-gypsum ratio, strength properties, and water resistance of high-strength gypsum binders. It was found that adding a single-component additive specifically to enhance water resistance does not significantly impact these properties. Complex additives have been developed based on Portland cement, granulated blast furnace slag, electric furnace slag, expanded clay dust, and granite screenings of various fractions. These additives are designed to maximize the water resistance of high-strength gypsum binder based on synthetic calcium sulfate dihydrate. As a result, the water resistance coefficient increased from 0.45 to 0.52. Additionally, a technological block diagram of the process has been proposed.

1 | Introduction

Incorporating industrial waste with diverse chemical compositions into the economy is a critical global issue [1–3]. Recycling and reusing waste conserves natural resources and lessens the environment harm [4–6]. In particular, although natural gypsum is essential for various building materials, numerous countries lack deposits. However, the production of high-quality gypsum and related binders can be obtained from various calcium-containing wastes [7–9].

Synthetic gypsum is a material obtained from industrial waste, mainly in countries that do not have their own deposits of natural gypsum. This material is widely used in construction and cement production, which helps to reduce the negative impact on the environment due to waste disposal [10]. Various methods for obtaining synthetic gypsum from different types of waste are discussed in the literature. Phosphogypsum is one of the most common types of waste used to produce synthetic gypsum [11]. This material is a by-product of the production of phosphoric acid from phosphate rocks. Phosphogypsum contains impurities

This is an open access article under the terms of the [Creative Commons Attribution](https://creativecommons.org/licenses/by/4.0/) License, which permits use, distribution and reproduction in any medium, provided the original work is properly cited.

© 2024 The Author(s). *Engineering Reports* published by John Wiley & Sons Ltd.

such as phosphates and rare earth elements, which requires pre-treatment before its use. However, many studies have shown that phosphogypsum can be successfully used to produce gypsum building materials after processing and purification [12]. Flue gas desulfurization gypsum is formed as a result of cleaning the exhaust gases of thermal power plants [13]. This synthetic gypsum has high purity and quality, which makes it attractive for use in the construction industry. Literature confirms that desulfogypsum can be used with little or no additional processing, reducing production costs [14]. Fluorogypsum is a by-product of the production of fluorine-containing chemicals such as hydrofluoric acid. Studies have shown that fluorogypsum can be recycled into gypsum building materials, although careful management of the fluorine content is required to avoid negative health effects [15]. Titanium gypsum is a waste product formed during the production of titanium dioxide. This type of waste can also be used to produce synthetic gypsum, although careful pre-treatment is necessary due to the presence of various impurities such as acids and metals [16]. Interest in recycling such waste has increased in recent years due to the increased production of titanium dioxide. Sulfur obtained during the refining of petroleum products can also be used to produce synthetic gypsum. This material, called sulfur gypsum, has good properties for use in construction, especially in regions with high sulfur content in petroleum refining waste. Synthetic gypsum from waste water treatment is a relatively new area of research that is promising due to the large volumes of waste generated during water treatment and its relative purity. These wastes typically include sediments containing calcium, magnesium, iron, aluminum, and other substances that can be recycled into useful materials.

Promising sources of calcium-containing wastes for synthetic gypsum production and binders on its base includes those from water treatment processes, such as coagulation sediments, lime mud, and sludge from water desalination using membrane filters. The precipitates formed from desalting of water on membrane filters, followed by evaporation, are primarily composed of calcium, sodium, and magnesium sulfates. The solubilities of the sulfates are as follows: $\text{CaSO}_4 \cdot \text{H}_2\text{O}$ —2.036 g/L, MgSO_4 —35.1 g/L, Na_2SO_4 —19.2 g/L [17]. Given their varying solubilities, a method of separation can be proposed. By evaporating the initial solution, gypsum can be isolated from the mixture containing sodium, magnesium, and calcium sulfates. The mass content ratio of the components is $\omega(\text{Na}_2\text{SO}_4) > \omega(\text{MgSO}_4) > \omega(\text{CaSO}_4)$. The composition of the resulting mixture resembles that of natural minerals containing sodium sulfate mixed with other sulfates, such as astrakhanite ($\text{Na}_2\text{SO}_4 \cdot \text{MgSO}_4 \cdot 4\text{H}_2\text{O}$) and glauberite ($\text{Na}_2\text{SO}_4 \cdot \text{CaSO}_4$). However, since the evaporation plant operates continuously, this method of separation is not feasible. As a result, gypsum extraction must occur from the resulting waste, or the waste must be utilized directly.

Calcium sulfate, found in the waste, is extensively used in construction products such as dry plaster, slabs and panels for partitions, gypsum stones, and architectural details. Gypsum-based products are characterized by relatively low density, fire resistance and low thermal conductivity. Additionally, calcium sulfate is used in medicine and art, where anhydrous calcium sulfate serves as a desiccant due to its hygroscopic properties. By integrating special additives, enhanced features can be incorporated. For instance, incorporating cobalt chloride

into Drierite, an anhydrous calcium sulfate desiccant, allows timely monitoring of the desiccant as it changes from blue to pink upon depletion [18]. Artificial calcium sulfate crystals, when doped with manganese or samarium, are also employed as thermoluminescent materials [19].

Sodium sulfate is primarily used in large quantities for manufacturing laundry detergents. It also plays a crucial role in glass production by serving as a clarifier [20]. In addition, it is utilized extensively in the production of cellulose via the sulfate process [21, 22], as well as in the textile [23], leather [24], and non-ferrous metallurgy industries [25]. In chemical laboratories, despite being slower than magnesium sulfate in dehydration, sodium sulfate is employed as a dehydrating agent due to its low price and ease of filtration.

Magnesium sulfate, on the other hand, is used as an additive in road constructions, airfield bases, and coatings [26]. It is also a component of magnesium cement [27], and in the pulp and paper industry, often serves as a filler [28] and helps maintain and enhance the physical and mechanical properties of paper, especially when bleaching agents like chlorines are used. Meanwhile, also used to prepare fire-resistant paper products and compositions for impregnations of various materials [29]. Additionally, it is utilized in the production of synthetic detergents [30], as a stabilizer for peroxide compounds, and widely in the textile industry as a filler, a weighting agent for silk and cotton, a mordant for dyeing, and as a bleaching agent [31].

A promising approach involves isolating calcium sulfate for use in building materials production, while the residual mixture containing sodium, magnesium, and calcium sulfates is thermally treated to remove crystalline moisture for use as a desiccant in laboratories and damp environments. Each component of this salt mixture can also be utilized as fertilizers [32], given that these substances arise from water treatment and are free from heavy metals. The potential applications of this waste are illustrated in Figure 1, with a focus on the annual production volume of 845.99 tons at a typical metalworking enterprise.

When manufacturing gypsum, it must adhere to the standards outlined in GOST 4013-2019. GOST specifies four grades of gypsum. For instance, binders are produced using grade 1 gypsum, which requires a minimum content of 95% $\text{CaSO}_4 \cdot 2\text{H}_2\text{O}$. Meanwhile, the $\text{CaSO}_4 \cdot 2\text{H}_2\text{O}$ content in grade 4 gypsum must be at least 70%.

Waste recycling is a key aspect of sustainable development, green chemistry [33, 34] and circular economy [35, 36]. Numerous industries have effectively incorporated waste usage into their processes, such as the production of pigments [37], materials for wastewater treatment [38–41], and various building materials including gypsum [42, 43], binders [9, 44], building blocks [45–49], and composite materials [50–53]. Gypsum-based materials, in particular, are valued for their performance characteristics and energy-efficiency during production. However, a major challenge with gypsum binders is their poor water resistance. Water-resistant gypsum binders could potentially replace Portland cement in many construction applications, offering rapid curing time and reduced energy consumption. Additionally, the presence of sodium ions in sludge from water

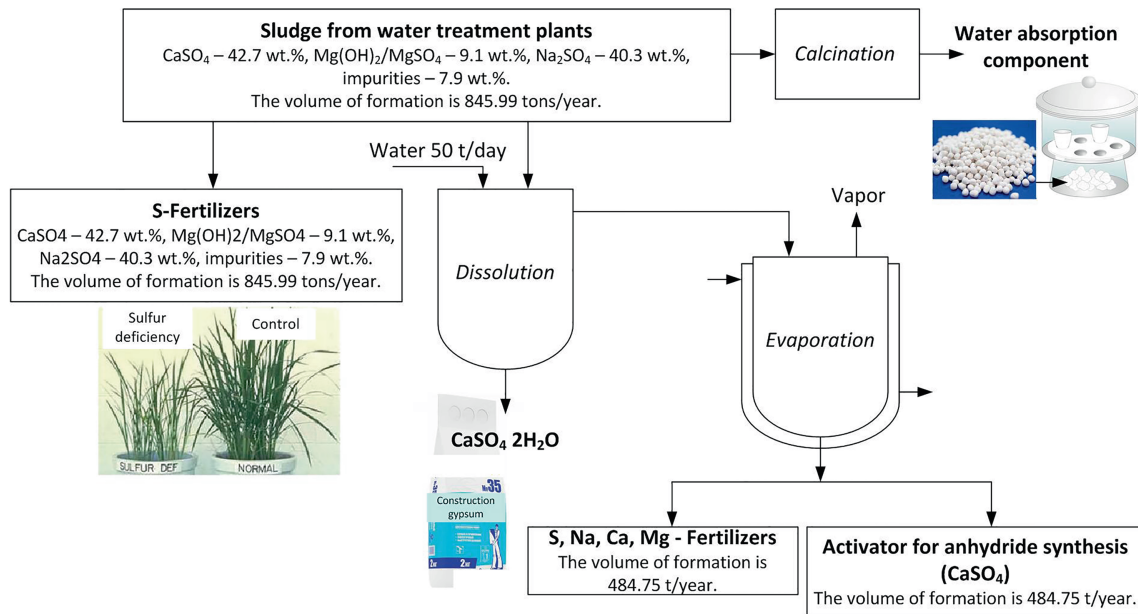


FIGURE 1 | Scheme of options for utilizing water treatment sludge.

treatment plants presents an opportunity to enhance the water resistance of these materials, thereby expanding their usability in building products and structures.

Therefore, the primary objectives of this work were: (1) To assess the feasibility of producing gypsum from the sludge generated at the neutralization station of a water treatment facility; (2) To evaluate the enhancement of water resistance in gypsum binder derived from waste, facilitated by the presence of sodium and the addition of other additives; (3) To explore the potential for using waste materials from various industries as additives that improve water resistance; (4) To develop a technological flow diagram for the process of extracting calcium sulfate from waste produced by water desalination using membrane filters; (5) To formulate strategies for utilizing waste streams effectively.

2 | Materials and Methods

2.1 | Materials and Reagents

The waste generated is a mixture, predominantly comprising calcium and sodium sulfates. This sludge originates from neutralization stations during the water treatment process of the tinplate manufacturing plant. This type of waste belongs to hazard class 4. Waste composition according to the average collected and provided by tinplate manufacturing plant (by combined SEM and XRD analysis): CaSO_4 —42.7 wt.%, MgSO_4 —9.1 wt.%, Na_2SO_4 —40.3 wt.%, impurities—7.9 wt.%. The volume of formation is 845.99 tons/year.

The selection of additives for producing binders from the resulting synthetic gypsum was primarily guided by the goal of maximizing the use of local raw materials, by-products, and industrial waste. The following mineral additives were used: Portland cement type CEM I 42.5 (Portland cement without

mineral additives, produced on the basis of clinker of standardized mineralogical composition with a limited content of tricalcium aluminate, manufactured by the Belarusian Cement Company), granulated blast furnace slag, electric furnace slag—metallurgical plant waste, expanded clay dust and granite screenings of 0.1–0.2 μm , synthetic gypsum. The detailed composition of these components is presented in the [Supporting Information](#) file.

2.2 | Preparation of High-Strength Gypsum Binder Based on Calcium Sulfate Dihydrate

Gypsum was obtained by dissolving sodium and magnesium sulfates. The solubility of the components decreases in the order $\omega\%(\text{Na}_2\text{SO}_4) > \omega\%(\text{MgSO}_4) > \omega\%(\text{CaSO}_4)$. The separation of sulfates by solubility was carried out using water in an amount of 1 L per 50 g of waste (this volume is close to the experimental solubility of the materials presented in the waste sample) and 1.2 L per 50 g of waste (20% exceed of the volume of water that is close to the experimental solubility of the materials presented in the waste sample). As a result, a solution of predominantly sodium and magnesium sulfates was formed, with an admixture of calcium sulfate, as well as undissolved calcium sulfate.

High-strength gypsum is produced using the autoclave method [54]. For the research, briquettes were prepared in the form of cylinders with dimensions: $h = 0.01$ m and $d = 0.02$ m. The main technological stages are: briquetting of powdered synthetic calcium sulfate dihydrate using a hydraulic press at a pressing pressure of 10–35 MPa. The density of the resulting samples was determined without correction for humidity using the formula:

$$\rho = m/V, \quad (1)$$

where m is the briquette mass, kg; V is the briquette volume, m^3 .

Autoclaving was carried out at a temperature of 130°C–150°C and an excess pressure of 0.4–0.6 MPa. Hydrothermal treatment

consists of three stages: pressure build-up for 1.5 h, isothermal exposure for 3–5 h (depending on what brand of gypsum binder we plan to obtain) and release (bypass) of steam for 1.5 h. After autoclaving, the briquettes were sent for drying at a temperature of 120°C–140 for 1.5–3 h. Next comes the stage of crushing the briquettes and grinding them to the required fineness based on the EN 13279-1:2008 standard [55]. High-strength gypsum binder is produced according to the following reaction:



2.3 | Analysis of the Composition and Properties of Binding Materials

The obtained samples of synthetic calcium sulfate hemihydrate and the resulting binders based on it were analyzed for the following indicators: normal density measurements were conducted according to the standard GOST 23789-2018 [56]; measuring setting time using a Vicat apparatus; determination of the compressive strength of samples measuring 20 × 20 × 20 mm was measured on a universal testing machine “Instron 1195” (GOST 1497-84 [57]).

A more detailed description of the methods is presented in the Supporting Information file.

2.4 | Analysis of Phase and Elemental Composition, Study of Surface Morphology

The phase composition of the solid phase was determined using a D8 ADVANCE X-ray diffractometer from Bruker (Germany). PDF4 2015 and DIFFRACPLUS software from Bruker were used to identify crystalline phases. The diffraction pattern profile was processed using HighScorePlus software.

The surface morphology and elemental composition of the surface of the samples was carried out on a JEOLJSM-5610LV

scanning electron microscope, equipped with a chemical micro-X-ray spectral analysis system.

3 | Results and Discussion

3.1 | Preparation of Calcium Sulfate Dihydrate

The SEM image (Figure 2a) shows that the aggregates of the provided sample of sludge from neutralization stations of the water treatment process represent a mixture of different phases with corresponding crystals of different shapes. XRD analysis shows (Figure 2b) the presence of $\text{CaSO}_4 \cdot 2\text{H}_2\text{O}$ phase with monoclinic crystal system and $C12/m1$ space group, MgSO_4 phase with orthorhombic crystal system and $Pnma$ space group, and Na_2SO_4 phase with orthorhombic crystal system and $Fddd$ space group.

The separation of sulfates by solubility was carried out using water in an amount of 1 L per 50 g of waste (Experiment 1) and 1.2 L per 50 g of waste (Experiment 2). As a result, a solution of predominantly sodium and magnesium sulfates was formed, with an admixture of calcium sulfate, as well as undissolved calcium sulfate. The compositions of the evaporated filtrate and undissolved gypsum are presented in Table 1.

According to the results obtained, the composition of the resulting gypsum includes about 5 wt.% impurities (experiment 1 and 2). It follows from this that the resulting gypsum (experiment 1 and 2) corresponds to grade 1 according to (GOST 4013-2019 [58]). Since dissolved Na and Mg compounds are very valuable for use as microfertilizers [59], the production of synthetic gypsum is carried out according to experiment 2.

As can be seen from Table 1, the filtrate, as expected from the analysis of the solubility of substances, contains predominantly sodium sulfate, with admixtures of magnesium and calcium sulfate. This determines the prospects of using it as a fertilizer.

The XRD results showed that the peaks fully correspond to gypsum and the calcium sulfate hemihydrate obtained from it

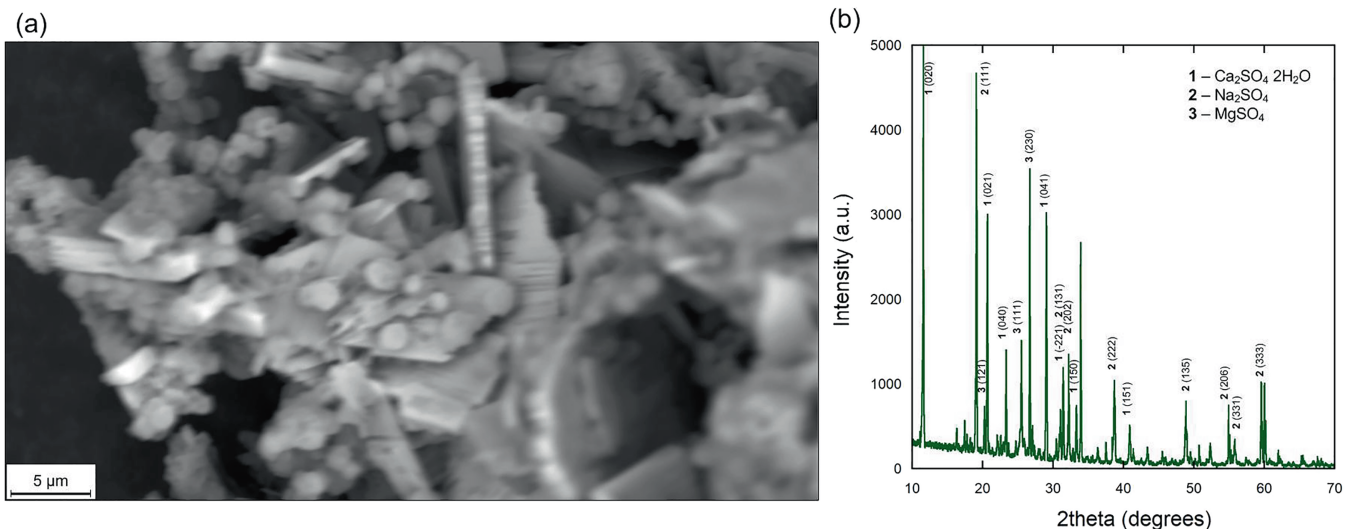


FIGURE 2 | SEM (a) and XRD (b) of the provided sample of sludge from neutralization stations of the water treatment process.

TABLE 1 | Elemental composition of the dry residue of the filtrate and gypsum.

Element	Experiment 1		Experiment 2	
	Dry residue	Gypsum	Dry residue	Gypsum
O	33.38 ± 0.04	42.85 ± 2.28	31.28 ± 0.16	43.52 ± 1.34
Na	35.01 ± 4.09	0.58 ± 0.48	35.23 ± 2.94	0.32 ± 0.18
Mg	4.10 ± 3.04	4.95 ± 0.39	5.44 ± 1.26	1.84 ± 0.79
S	25.01 ± 1.73	14.51 ± 0.20	24.90 ± 2.34	15.26 ± 1.33
Ca	2.51 ± 0.71	37.11 ± 1.22	3.15 ± 1.23	38.95 ± 1.16

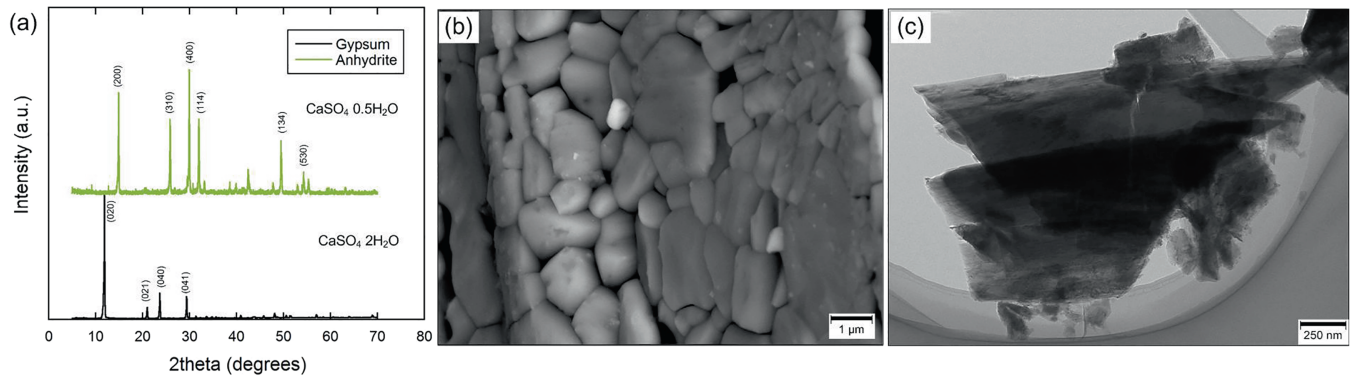


FIGURE 3 | XRD of (a) gypsum and high-strength gypsum binder obtained from synthetic gypsum; SEM (b) and TEM (c) images of obtained binder.

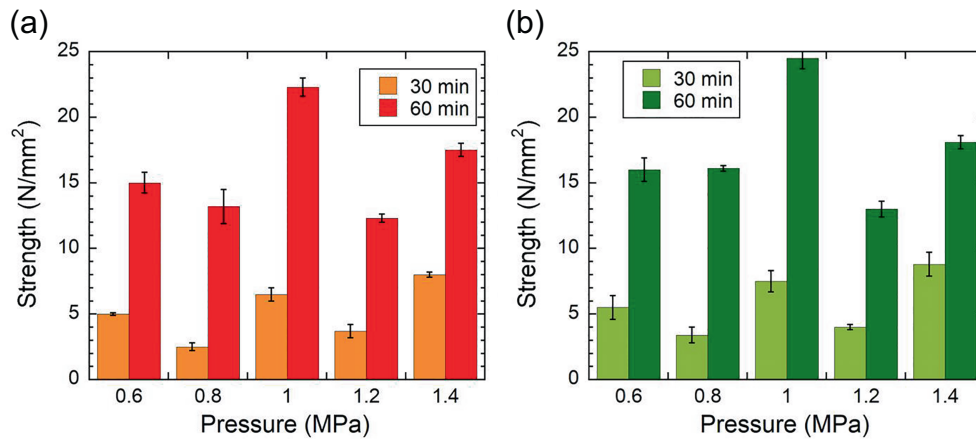


FIGURE 4 | Strength characteristics of gypsum binders depending on autoclave processing parameters.

(Figure 3a). Figure 3b,c show SEM and TEM images of the resulting calcium sulfate hemihydrate.

The material balance of obtaining gypsum from sludge from a neutralization station during wastewater treatment is presented in Table S1. According to the elemental composition, the resulting gypsum has 95 wt.% of the main substance, and about 8 wt.% of gypsum from the original mass remains in the filtrate after separating the mixture. The centrifuge, due to the size of the mesh cell, can provide a gypsum moisture content of 8–12 wt.%. When calculating, we assume the moisture content of the resulting synthetic gypsum is 10 wt.%. Composition of waste used for mass balance calculations: Na_2SO_4 –40.3 wt.%; $\text{CaSO}_4 \cdot 2\text{H}_2\text{O}$ —50.6 wt.%; MgSO_4 –9.1 wt.%. The calculation was carried out for 1000 kg of the initial mixture.

3.2 | Preparation of High-Strength Gypsum Binder From Gypsum

The material balance for obtaining gypsum binder from the resulting gypsum is presented in Table S2. This part of research has been carried out on the production of gypsum binders using the autoclave method. The dependence of the influence of autoclaving pressure and isothermal exposure time on the strength properties of gypsum binder was established. Data on the strength characteristics of the obtained gypsum binders depending on the autoclaving pressure are presented in Figure 4.

During the research, the dependence of autoclaving pressure on the yield of $\text{CaSO}_4 \cdot 0.5\text{H}_2\text{O}$ was established. At an autoclaving pressure of 0.6 MPa for 30 min, calcium sulfate dihydrate is

present in the sample in an amount of 5 wt.%. At excess pressure at 1.4 MPa for 30 and 60 min, the $\text{CaSO}_4 \cdot 2\text{H}_2\text{O}$ phase remains in the amount of 1 and 2 wt.%, respectively, and the anhydrite phase at 60 min in the amount of 9 wt.%. The presence of phases other than the semi-aqueous form will affect the strength properties. Thus, to obtain gypsum binder with the highest strength characteristics, an autoclaving mode with exposure for 30 min at a pressure of 1.0 MPa is suitable. Also, high strength indicators were shown by the material obtained by holding for 60 min at a pressure of 1.4 MPa. However, due to the higher steam consumption to maintain pressure in the autoclave (1.4 MPa), this method is not competitive in comparison with the 60 min mode at a pressure of 1.0 MPa.

The final stage of obtaining high-strength gypsum binder is its drying. Dehydration and recrystallization during hydrothermal treatment of dense briquettes of calcium sulfate dihydrate changes the structure of the material, transforming it from dense to capillary-porous with a highly developed internal surface. Water, which is intensively removed from the material when the pressure in the autoclave is reduced, partially remains in the pores of the material. The possibility of hydration of semi-aqueous gypsum in this case can lead to significant unevenness of the resulting material in composition, which will affect the main technical characteristics of the binder.

To study the drying parameters for the quality of the binder, the material steamed according to the optimal regime was subjected to heat treatment in a drying cabinet; at the same time, the

temperature was varied in the range from 70°C to 150°C and the drying time from 60 to 120 min. At the end of the drying process, the material was subjected to grinding, after which the content of hydration water in the product and its physical and mechanical properties were determined [60].

One of the important technological operations is the drying stage, which is carried out after the autoclaving process. At this stage, the possibility of the hydration reaction of calcium sulfate hemihydrate is excluded. The results of the studies are presented in Table 2.

Analysis of the results obtained shows that drying at temperatures from 70°C to 90°C for any duration of the process leads to the formation of secondary calcium sulfate dihydrate in the product; the content of hydration water in it ranges from 11.0% to 19.4%, which corresponds to the content of $\text{CaSO}_4 \cdot 2\text{H}_2\text{O}$ in an amount from 35% to 80%. Raising the temperature to 90°C already significantly improves the quality of the binder, and when the steamed material was kept in a drying cabinet for 30 min, its phase composition is represented exclusively by calcium sulfate hemihydrate.

The material contains up to 5% $\text{CaSO}_4 \cdot 2\text{H}_2\text{O}$, which significantly worsens the physical and mechanical properties of the binder: setting time is reduced, the water-gypsum ratio is increased, and the compressive strength is reduced. However, after drying at 120°C for 100–150 min, the material is already represented exclusively by calcium sulfate hemihydrate. At the same time,

TABLE 2 | Effect of drying time and temperature on the composition, strength and water requirement of gypsum binder.

Temperature, °C	Time, min	Content, wt.%			W/G	Strength, MPa
		$\text{CaSO}_4 \cdot 2\text{H}_2\text{O}$	$\text{CaSO}_4 \cdot 0.5\text{H}_2\text{O}$	CaSO_4		
60	30	80	20	0	0.53	7.7
	60	78	22	0	0.53	8.3
	90	77	23	0	0.53	8.6
	120	77	23	0	0.53	8.6
	150	76	24	0	0.53	8.8
90	30	70	30	0	0.52	10.6
	60	62	38	0	0.51	12.4
	90	55	45	0	0.49	15.0
	120	43	57	0	0.48	17.1
	150	35	65	0	0.48	17.9
120	30	31	69	0	0.48	18.3
	60	18	82	0	0.47	19.8
	90	9	91	0	0.46	21.0
	120	3	97	0	0.45	21.8
	150	1	99	0	0.45	22.3
150	30	27	73	0	0.48	18.7
	60	13	82	5	0.47	19.7
	90	7	80	13	0.47	19.5
	120	2	70	28	0.48	18.3
	150	1	64	35	0.49	17.9

binders have maximum strength and minimum water requirement. However, a further increase in the drying temperature to 150°C leads to the formation of insoluble anhydrite in the product, which reduces the strength of the binder and lengthens the setting time.

Thus, the material can be heat treated after steaming in a fairly wide temperature range (from 80°C to 150°C). A higher temperature speeds up the drying process significantly.

It is believed that there is clear relationship between the strength of the hardened material and the size of its constituent crystals; the conditions for the growth of these crystals play a decisive role [61]. It is also known that the formation of the gypsum structure is influenced by such mixing parameters as the specific surface area of the binder, the water-gypsum ratio, the temperature of the mixing water, relative air humidity, etc. [62]. There is no consensus on the influence of these factors on the hardening process of gypsum.

One of the most important parameters is the particle size of the gypsum binder. To study the effect of this indicator on the strength of the hardened material, dried gypsum washers were ground for 5–20 min.

In addition, the fact that the compressive strength of the binder increases with increasing particle size can be explained by the fact that with a decrease in the dispersion of the binder, the supersaturation of the gypsum solution during hydration increases due to better solubility of gypsum crystals, which leads to an increase in the number of surface intergrowth contacts between the crystals, and, consequently, to increase the strength of hardened gypsum [61, 63]. When grinding the binder beyond the optimal value, aggregation of powder particles occurs, which causes an increase in the water demand of the binder, and this, in turn, negatively affects its strength properties. In this case, a lot of water is blocked in the macropores of the hardening system, which, when the hardened gypsum dries, reduces its volumetric mass and softens the structure.

The dispersion of the binder is an important technical characteristic of high-strength gypsum binder and allows you to adjust its physical and mechanical properties over a wide range. The optimal grinding time is grinding for 20 min, since the residue on sieve No. 02 was 15 wt.%, which meets the requirements of the standard for gypsum binders [60]. When grinding for 25 min, the residue on sieve No. 02 increases from 15 to 21 wt.% this is due to the agglomeration process of crushed particles that occurs in the mill. The resulting fine particles form secondary agglomerates.

3.3 | Properties of the Resulting Gypsum Binder

Gypsum binders are characterized by the following properties: mechanical strength, setting time, grinding fineness, specific surface area, water requirement, density, color, etc. Based on them, you can evaluate the quality and scope of gypsum binders.

The setting time is determined by the time from the moment the gypsum binder is mixed with water until the beginning and end of setting. They depend on the material (modification) composition of the binder. Rapid setting is characteristic of binders consisting

TABLE 3 | Types of gypsum binders depending on setting time.

Type of binder	Curing time index	Setting time, min	
		Start, not earlier	End, no later
Fast-hardening	A	2	15
Normal hardening	B	6	30
Slow-hardening	C	20	Not standardized

mainly of α -CaSO₄·0.5H₂O and β -CaSO₄·0.5H₂O. Anhydrite binders, on the other hand, set slowly.

In addition, the setting time is influenced by the fineness of grinding, the water-gypsum ratio, the duration and storage conditions and other factors. The finer the grinding of the binder, the shorter the setting time, and an increase in storage duration causes them to increase [62].

According to the setting time, gypsum binders are divided into fast-hardening, normal-hardening and slow-hardening, the data is given in Table 3.

The binder obtained by the method described above is characterized by the following setting times: start 6–7 min, end 13–14 min, which meets the requirements of regulatory and technical documentation for high-strength gypsum binders. If it is necessary to regulate the setting time over a wider range of times, additives can be used.

Experimentally, according to the standard EN, B. 13279:2014 [64], based on the diameter of the dough spread, which was 181 mm, the water-gypsum ratio for the resulting gypsum binder was established, which was 0.43, which meets the requirements of the standard for high-strength gypsum binder.

The water resistance of gypsum binders is characterized by the softening coefficient (K_p), which is the ratio of the strength of the samples after keeping them in water (R_w) to the strength in a dry state (R_c)

$$K_p = R_w/R_c \quad (2)$$

The value of K_p is for different gypsum binders in a fairly wide range from 0.2 to 0.9 and above. According to water resistance, they are divided into: non-waterproof $K_p < 0.45$; average water resistance $0.45 \leq K_p \leq 0.6$; increased water resistance $0.6 < K_p \leq 0.8$; waterproof $K_p > 0.8$. The resulting gypsum binder is a medium water-resistant binder with $K_p = 0.55$.

3.4 | High-Strength Gypsum Binder With Increased Water Resistance

Previous studies [8] on the influence of various compositions of additives on increasing the water resistance of high-strength gypsum binder based on synthetic gypsum obtained from calcium-containing water treatment waste allowed us to establish eight compositions (Table 4) that allow obtaining maximum values of the water resistance coefficient.

TABLE 4 | Content of components in gypsum binder samples and their characteristics.

Composition	Content of additive, wt. %							W/G	Ultimate compressive strength R_{com} , MPa at the age of 7 days	K_p
	High-strength gypsum binder	Blast furnace slag	Granite screenings	Portland cement	Electric steel smelting slag	Expanded clay dust				
Sample 1	75	20	5	—	—	—	—	0.57	17.4	0.76
Sample 2	75	—	5	20	—	—	—	0.56	17.8	0.78
Sample 3	75	—	5	—	20	—	—	0.52	19.4	0.81
Sample 4	80	20	—	—	—	—	—	0.56	11.6	0.68
Sample 5	80	—	—	—	20	—	—	0.51	10.9	0.65
Sample 6	80	—	20	—	—	—	—	0.52	10.9	0.60
Sample 7	80	—	—	—	—	20	—	0.53	8.9	0.53
Sample 8	80	—	—	20	—	—	—	0.55	9.7	0.68
Sample 9	100	—	—	—	—	—	—	0.45	22.3	0.55

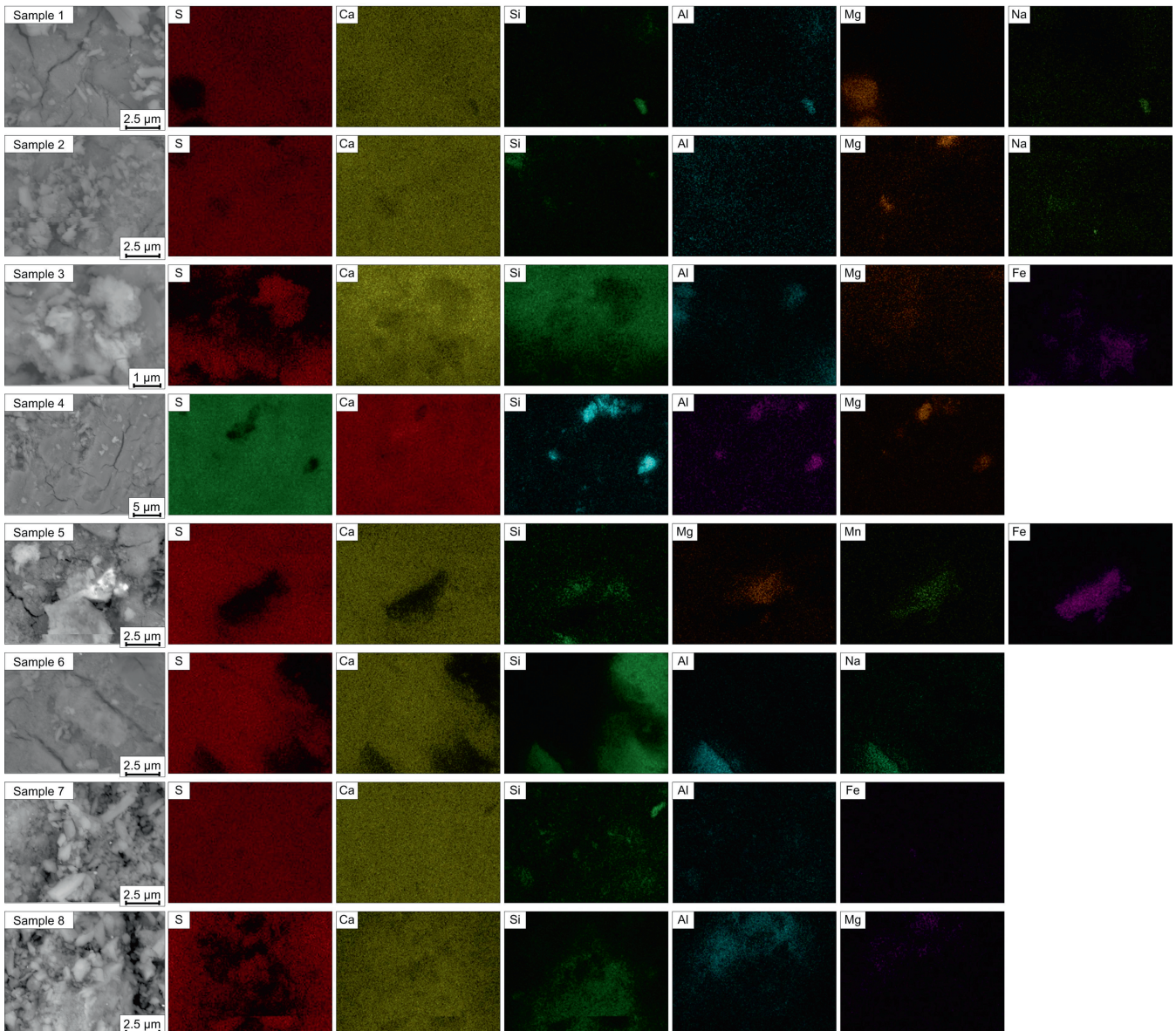


FIGURE 5 | SEM-EDS maps of samples 1–8 with increased water resistance.

Sample 1 displays a dense matrix with dispersed bright spots, and a homogeneous distribution of Ca and Al, while S and Mg are localized and Na is sparse. Sample 2 has a more porous structure, with uniform S and Ca, widespread Al, and concentrated Mg and Na. Sample 3 features agglomerated particles, scattered S and Ca, prominent Fe, and clustered Mg. Sample 4 appears more porous, with well-distributed S, some concentrations of Si and Al, less uniform Mg, and discrete Fe. Sample 5 has larger aggregates and a rough surface, with evenly spread S and Ca, and distinct Mn and Fe concentrations. Sample 6 is similarly porous, with evenly distributed S and Ca, but less prominent Na and Mg. Sample 7 shows a fine granular structure with uniform S and Ca, and concentrated Fe, suggesting compositional differences. Sample 8 has a relatively smooth surface with small agglomerates, uniform S and Ca, and scattered Fe and Al. Both samples 7 and 8 are most porous and shown similar lower ultimate compressive strength. Overall, the elemental maps reveal varying compositions and distributions across the samples as different additives were added,

with notable differences in Fe and Mg concentrations. The optimal composition to obtain a material with a water resistance coefficient of 0.81 was 20 wt.% electric furnace slag and 5 wt.% granite screenings (composition 3). With the introduction of these additives, the strength indicators of the material decrease by only 13% from the initial strength indicators of the gypsum binder. This indicator of the water resistance coefficient of composition 3 is achieved due to the uniform dense distribution of compounds of the elements Si, Al, and Fe throughout the material (Figure 5).

3.5 | Scheme for Producing Synthetic Gypsum and Gypsum Binders From Membrane Water Desalination Wastes

Based on the experiment, the following scheme was proposed for processing the waste under study into gypsum and gypsum binders (Figure 6). Sludge from neutralization stations is dosed from hopper 1 into reactor 2. Then water is added to the reactor

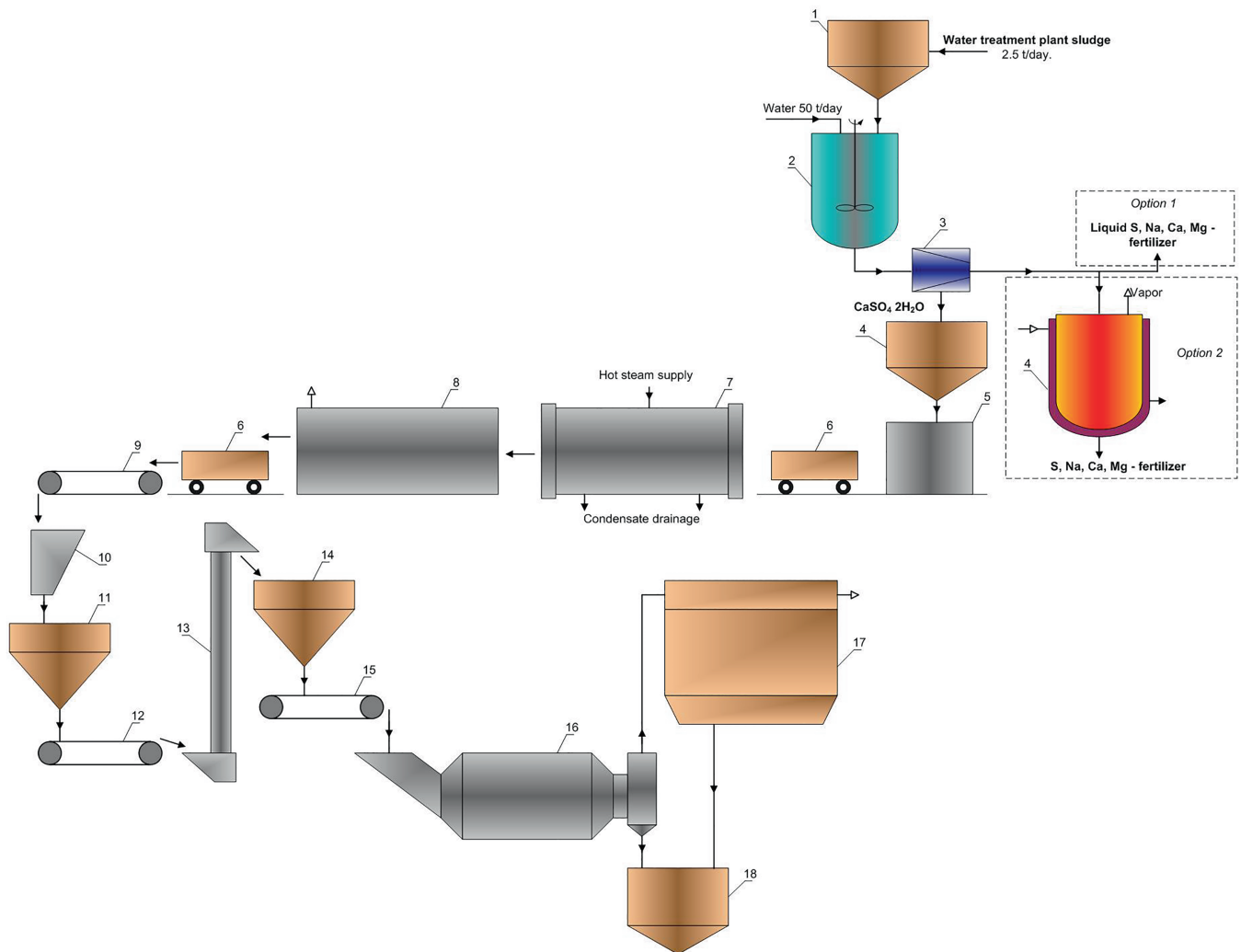


FIGURE 6 | Technological scheme for the production of high-strength gypsum binder.

with constant stirring with a stirrer. After dissolving the salts, the resulting suspension enters centrifuge 3 to be separated into gypsum and filtrate, which contains predominantly soluble sulfates. According to the first option, the resulting filtrate can be used as a liquid fertilizer. According to the second option, the filtrate can be evaporated and crystallized to obtain bulk fertilizer.

Recommended parameters when implementing the scheme:

- dissolution of sulfates—25 L of water per 1 kg of sludge on a dry matter basis;
- dissolution time—60 min with constant stirring.

The production of high-strength gypsum binder is the most promising direction for processing the resulting synthetic calcium sulfate dihydrate based on technogenic raw materials (sludge from a membrane water desalination station). High-strength gypsum, due to its superior grade, enables the creation of a broader range of gypsum-based materials. Additionally, these high-grade materials can be converted to lower grades through dilution if necessary, offering flexibility in their use.

The technological process for the production of high-strength gypsum binder (Figure 4) includes the following stages:

- briquetting of synthetic gypsum;
 - hydrothermal treatment of calcium sulfate dihydrate to produce α - $\text{CaSO}_4 \cdot 0.5\text{H}_2\text{O}$ by the reaction:
- $$\text{CaSO}_4 \cdot 2\text{H}_2\text{O} = \text{CaSO}_4 \cdot 0.5\text{H}_2\text{O} + 1.5\text{H}_2\text{O} \quad (3)$$
- crushing briquettes of calcium sulfate hemihydrate;
 - drying of crushed calcium sulfate hemihydrate;
 - grinding of material;
 - warehousing.

Synthetic gypsum is fed into the hopper (pos. 4). The material is briquetted on a hydraulic press (pos. 5) at a pressing pressure of 20–25 MPa. The volumetric mass of the compressed briquette is about 1.7 g/cm³. Next, calcium sulfate dihydrate briquettes on trolleys (pos. 6) are sent for dehydration to an autoclave (pos. 7) at an operating pressure of 1.2 MPa.

The autoclaving process is divided into 3 main stages:

1. raising the pressure of saturated water vapor and temperature to operating parameters: 30–40 min;
2. isothermal exposure at constant pressure and temperature: 3 h;
3. pressure reduction and steam release: 30–40 min.

To carry out hydrothermal treatment, a periodic apparatus was selected (based on the practice of use both in small-scale production and in large-scale technologies).

After the hardening process is completed and the pressure in the autoclave is released, it is opened. Autoclave trolleys connected to each other in a train are pulled out of the autoclave. After unloading from the autoclave, the dehydrated gypsum is quickly fed into the tunnel dryer (pos. 8). Briquettes are dried by combustion products of natural gas at a temperature of 115°C–120°C to constant weight.

Next, the dried material is fed to the jaw crusher (pos. 10) using a belt conveyor (pos. 9). Crushing continues for 10–15 min to pieces 1–3 cm in size. The crushed material enters the hopper (pos. 11), then using a belt conveyor (pos. 12) through an elevator (pos. 13) is fed into the supply hopper (pos. 14), after which the belt feeder (pos. 15) feeds it into a two-chamber ball mill (pos. 16). Grinding continues for 35–40 min, after which the contents of the mill are unloaded into the hopper (pos. 18).

Dusty air from the ball mill passes through a bag filter (pos. 17). The collected dust of material in the bag filter is fed into the hopper (pos. 18). Gypsum binder from the hopper (pos. 18) is supplied to the packaging installation and then shipped to the consumer.

This production is medium-tonnage, therefore, measures for the mechanization of loading and unloading operations are not provided.

3.6 | Assessment of the Possibility of Using the Obtained Products at Construction Materials Production Enterprises

Previously, studies were carried out on the possibility of using synthetic gypsum from calcium-containing water treatment waste in the production of an expanding additive of the sulfoaluminate type RSAM, used to compensate for the shrinkage of freshly laid concrete. The introduction of the PSAM modifier in the process of preparing a concrete mixture regulates the expansion energy of the binder, which makes it possible to obtain concrete for prefabricated and monolithic construction, both with compensated shrinkage and prestressing, with different self-stress energies. The possible consumption of synthetic gypsum for the production of PCAM additive is about 600 tons/year.

Synthetic gypsum can be used in the production of cement, replacing natural gypsum stone, which is used to regulate the setting time of cement. Gypsum is introduced into the process of

grinding cement clinker in an amount of up to 3 wt.% by weight of cement clinker.

Synthetic gypsum, due to its degree of purity, is a promising raw material for the production of gypsum binders based on it. Gypsum binders are the main raw material in the production of plasterboard sheets, tongue-and-groove boards and dry construction mixtures, as well as the creation of composite materials for various purposes.

4 | Conclusions

In the presented work, a technological block diagram of the process of processing a mixture based on calcium and sodium sulfates (code 3164400) was developed in order to obtain gypsum as the main product. It has been determined that due to the varying solubility of the components in water treatment waste—a mixture of calcium and sodium sulfates—it is possible to produce grade 1 gypsum in accordance with GOST 4013-2009 through a two-stage process involving dissolution and centrifugation. The resulting filtrate at pH 8.36 contains about 25 g/L of soluble sulfates, which can be used as a sulfate microfertilizer.

The resulting synthetic gypsum based on the model system belongs to grade I gypsum. This indicator allows us to consider it a promising material for the production of building materials (gypsum binders, Portland cement, etc.).

The high-strength gypsum binder obtained on the basis of synthetic gypsum of the model system meets all the standards prescribed in the standard for gypsum binders.

Gypsum binder generally has moderate water resistance, but this characteristic can be varied based on specific requirements. The water resistance coefficient of the binder can be enhanced by incorporating various additives, including complex formulations. Not all additives, in their pure form, can significantly enhance the water resistance of gypsum binder without adversely affecting its basic properties, however, it was possible to achieve $K_p = 0.6$ with the introduction of 20 wt.% granulated blast furnace slag and Portland cement PC 500 D0 with the least losses in terms of basic properties. The optimal composition of the complex additive is 20 wt.% electric furnace slag and 5 wt.% of granite screenings, which make it possible to increase the water resistance coefficient from 0.38 to 0.81 while reducing the strength indicators from only 22.3 to 19.14 MPa with a slight increase in the water-gypsum ratio from 0.45 to 0.52.

The results of biotesting using oil radish showed that when using filtrate for irrigation (dose of 2 mL per plant at initial concentration), the height of almost half of the sprouts increased to 37% compared to test irrigation with water, while the length of the main root for both samples was almost the same values.

Author Contributions

Valentin Romanovski: supervision, conceptualization, methodology, validation, investigation, formal analysis, data curation, visualization, writing – original draft, writing – review and editing. **Dmitry**

Moskovskikh: data curation, formal analysis. **Hongbin Tan:** formal analysis, data curation, writing – review and editing. **Kirill Kuskov:** investigation. **Sergey Volodko:** investigation. **Abayomi Adewale Akinwande:** data curation, formal analysis, investigation. **Rajiv Periakaruppan:** formal analysis, data curation. **Fanyue Kong:** investigation, writing – review and editing. **Xiaoling Ma:** data curation, formal analysis. **Feihua Yang:** data curation, formal analysis. **Maksim Kamarou:** methodology, validation, investigation, formal analysis, data curation, writing – original draft.

Ethics Statement

The authors have nothing to report.

Consent

The authors have nothing to report.

Conflicts of Interest

The authors declare no conflicts of interest.

Data Availability Statement

The data that support the findings of this study are available from the corresponding author upon reasonable request.

References

1. M. S. Wei and K. H. Huang, “Recycling and Reuse of Industrial Wastes in Taiwan,” *Waste Management* 21, no. 1 (2001): 93–97.
2. V. V. Ranade and V. M. Bhandari, “Industrial Wastewater Treatment, Recycling, and Reuse,” in *Industrial Wastewater Treatment, Recycling and Reuse* (Kidlington, Oxford: Butterworth-Heinemann, 2014).
3. J. Tang, Y. Liu, R. Y. Fung, and X. Luo, “Industrial Waste Recycling Strategies Optimization Problem: Mixed Integer Programming Model and Heuristics,” *Engineering Optimization* 40, no. 12 (2008): 1085–1100.
4. L. Ma, Y. Ghorbani, C. B. Kongar-Syuryun, et al., “Dynamics of Backfill Compressive Strength Obtained From Enrichment Tails for the Circular Waste Management,” *Resources, Conservation & Recycling Advances* 23 (2024): 200224.
5. V. S. Brigida, V. I. Golik, and B. V. Dzeranov, “Modeling of Coalmine Methane Flows to Estimate the Spacing of Primary Roof Breaks,” *Mining* 2, no. 4 (2022): 809–821, <https://doi.org/10.3390/mining2040045>.
6. K. W. Shen, L. Li, and J. Q. Wang, “Circular Economy Model for Recycling Waste Resources Under Government Participation: A Case Study in Industrial Waste Water Circulation in China,” *Technological and Economic Development of Economy* 26, no. 1 (2020): 21–47.
7. C. Wang, X. Ma, W. Zhong, et al., “Preparation of Calcium Sulfate From Recycled Red Gypsum to Neutralize Acidic Wastewater and Application of High Silica Residue,” *Journal of Material Cycles and Waste Management* 26 (2024): 1–8.
8. M. Kamarou, D. Moskovskikh, K. Kuskov, et al., “High-Strength Gypsum Binder With Improved Water-Resistance Coefficient Derived From Industrial Wastes,” *Waste Management & Research* (2024): 0734242X241240042, <https://doi.org/10.1177/0734242X241240042>.
9. M. Kamarou, D. Moskovskikh, H. L. Chan, et al., “Low Energy Synthesis of Anhydrite Cement From Waste Lime Mud,” *Journal of Chemical Technology & Biotechnology* 98, no. 3 (2023): 789–796.
10. M. N. V. Prasad, “Resource Potential of Natural and Synthetic Gypsum Waste,” in *Environmental Materials and Waste* (Kidlington, Oxford: Elsevier, 2024), 369–424.
11. L. Zhang, K. H. Mo, T. H. Tan, C. C. Hung, S. P. Yap, and T. C. Ling, “Influence of Calcination and GGBS Addition in Preparing β -Hemihydrate

Synthetic Gypsum From Phosphogypsum,” *Case Studies in Construction Materials* 19 (2023): e02259.

12. E. P. Lokshin and O. A. Tareeva, “Production of High-Quality Gypsum Raw Materials From Phosphogypsum,” *Russian Journal of Applied Chemistry* 88 (2015): 567–573.
13. N. H. Koralegedara, P. X. Pinto, D. D. Dionysiou, and S. R. Al-Abed, “Recent Advances in Flue Gas Desulfurization Gypsum Processes and Applications—A Review,” *Journal of Environmental Management* 251 (2019): 109572.
14. P. Tesárek, J. Drchalová, J. Kolísko, P. Rovnaníková, and R. Černý, “Flue Gas Desulfurization Gypsum: Study of Basic Mechanical, Hydric and Thermal Properties,” *Construction and Building Materials* 21, no. 7 (2007): 1500–1509.
15. M. E. Bazaldua-Medellin, R. X. Magallanes-Rivera, and J. E. Garcia, “Composite Hydraulic Binders Based on Fluorgypsum: Reactions, Properties and Sustainability,” *Journal of Building Engineering* 53 (2022): 104590.
16. X. Y. Li and J. Y. Yang, “Production, Characterisation, and Application of Titanium Gypsum: A Review,” in *Process Safety and Environmental Protection*, vol. 181 (2023), 64–74.
17. P. Glynn, “Solid-Solution Solubilities and Thermodynamics: Sulfates, Carbonates and Halides,” *Reviews in Mineralogy and Geochemistry* 40, no. 1 (2000): 481–511.
18. Dehumidifier Drierite, Date of access August 27, 2020, <https://labtech.com/pid34294/osushitel-drierite-s-indikatorom-8-mesh-vwr-23025/>.
19. M. Souli, M. Reghima, M. Secu, et al., “Physical Properties Investigation of Samarium Doped Calcium Sulfate Thin Films Under High Gamma Irradiations for Space Photovoltaic and Dosimetric Applications,” *Superlattices and Microstructures* 126 (2019): 103–119.
20. H. Rashidian-Dezfouli and P. R. Rangaraju, “A Comparative Study on the Durability of Geopolymers Produced With Ground Glass Fiber, Fly Ash, and Glass-Powder in Sodium Sulfate Solution,” *Construction and Building Materials* 153 (2017): 996–1009.
21. S. Beck, M. Méthot, and J. Bouchard, “General Procedure for Determining Cellulose Nanocrystal Sulfate Half-Ester Content by Conductometric Titration,” *Cellulose* 22 (2015): 101–116.
22. V. Zalyhina, V. Cheprasova, and V. Romanovski, “Paper Industry Slag for the Production of Building Ceramics,” *Journal of Chemical Technology & Biotechnology* 97, no. 11 (2022): 3091–3099.
23. F. M. Amaral, M. T. Kato, L. Florêncio, and S. Gavazza, “Color, Organic Matter and Sulfate Removal From Textile Effluents by Anaerobic and Aerobic Processes,” *Bioresource Technology* 163 (2014): 364–369.
24. P. S. Vankar, A. Dwivedi, and R. Saraswat, “Sodium Sulphate as a Curing Agent to Reduce Saline Chloride Ions in the Tannery Effluent at Kanpur: A Preliminary Study on Techno-Economic Feasibility,” *Desalination* 201, no. 1–3 (2006): 14–22.
25. A. V. Tarasov and V. A. Bocharov, “Technology for Separation of Non-ferrous Metal Minerals With Similar Physical and Chemical Properties,” in *Developments in Mineral Processing*, vol. 13 (2000), C9–C10.
26. S. Liu and Y. Tan, “Mechanical Properties and Water Resistance Study of Basic Magnesium Sulfate Cement-Emulsified Asphalt Composite Materials,” *Construction and Building Materials* 426 (2024): 136196.
27. X. Zeng, H. Yu, and C. Wu, “An Overview of Study on Basic Magnesium Sulfate Cement and Concrete in China (2012–2019),” *KSCE Journal of Civil Engineering* 23, no. 10 (2019): 4445–4453.
28. K. Mehmood, S. K. U. Rehman, J. Wang, et al., “Treatment of Pulp and Paper Industrial Effluent Using Physicochemical Process for Recycling,” *Water* 11, no. 11 (2019): 2393.

29. V. Colson, M. Bourebrab, M. Dalmais, O. Jadeau, and C. Lanos, "Formulation of Novel Fire Retardant Additives for Biobased Insulation Material," *Academic Journal of Civil Engineering* 37, no. 2 (2019): 134–141.
30. G. P. Edwards and M. E. Ginn, "Determination of Synthetic Detergents in Sewage," *Sewage and Industrial Wastes* vol. 26, no. 8 (1954): 945–953.
31. A. K. Verma, P. Bhunia, and R. R. Dash, "Decolorization and COD Reduction Efficiency of Magnesium Over Iron Based Salt for the Treatment of Textile Wastewater Containing Diazo and Anthraquinone Dyes," *International Journal of Materials and Textile Engineering* 6, no. 6 (2014): 365–372.
32. J. J. Mortvedt and J. J. Kelsoe, "Crop Response to Fine and Granular Magnesium Fertilizers," *Fertilizer Research* 15 (1988): 155–161.
33. W. R. Stahel, "The Circular Economy," *Nature News* 531, no. 7595 (2016): 435–438, <https://doi.org/10.1038/531435a>.
34. M. Nelles, J. Gruenes, and G. Morscheck, "Waste Management in Germany—Development to a Sustainable Circular Economy?," *Procedia Environmental Sciences* 35 (2016): 6–14, <https://doi.org/10.1016/j.proenv.2016.07.001>.
35. A. Pires and G. Martinho, "Waste Hierarchy Index for Circular Economy in Waste Management," *Waste Management* 95 (2019): 298–305, <https://doi.org/10.1016/j.wasman.2019.06.014>.
36. S. van Ewijk and J. A. Stegemann, "Recognising Waste Use Potential to Achieve a Circular Economy," *Waste Management* 105 (2020): 1–7, <https://doi.org/10.1016/j.wasman.2020.01.019>.
37. V. Zalyhina, V. Cheprasova, and V. Romanovski, "Pigments From Spent Chloride-Ammonium Zinc Plating Electrolytes," *Journal of Chemical Technology and Biotechnology* 96 (2021): 2767–2774, <https://doi.org/10.1002/jctb.6822>.
38. V. I. Romanovskii and V. N. Martsul, "Distribution of Heteroatoms of Synthetic Ion Exchangers in Pyrolysis Products," *Russian Journal of Applied Chemistry* 82, no. 5 (2009): 836–839, <https://doi.org/10.1134/S1070427209050164>.
39. V. I. Romanovskii and V. N. Martsul, "Functional Group Distribution Over the Surface and in the Bulk of Particles of Spent Ion Exchangers in the Course of Mechanochemical Destruction," *Russian Journal of Applied Chemistry* 85, no. 3 (2012): 371–376, <https://doi.org/10.1134/S1070427212030081>.
40. E. M. Bakhsh, S. B. Khan, K. Akhtar, et al., "Simultaneous Preparation of Humic Acid and Mesoporous Silica From Municipal Sludge and Their Adsorption Properties for U(VI)," *Colloids and Surfaces A: Physicochemical and Engineering Aspects* 647 (2022): 129060, <https://doi.org/10.1016/j.colsurfa.2022.129060>.
41. J. Zeng, R. Xu, A. A. El-Kady, et al., "Nanomaterials Enabled Photoelectrocatalysis for Removing Pollutants in the Environment and Food," *TrAC Trends in Analytical Chemistry* vol. 166 (2023): 117187.
42. M. Kamarou, N. Korob, and V. Romanovski, "Structurally Controlled Synthesis of Synthetic Gypsum Derived From Industrial Wastes: Sustainable Approach," *Journal of Chemical Technology and Biotechnology* 96, no. 11 (2021): 3134–3141, <https://doi.org/10.1002/jctb.6865>.
43. V. Romanovski, L. Zhang, X. Su, A. Smorokov, and M. Kamarou, "Gypsum and High Quality Binders Derived From Water Treatment Sediments and Spent Sulfuric Acid: Chemical Engineering and Environmental Aspects," *Chemical Engineering Research and Design* 184 (2022): 224–232.
44. M. Kamarou, N. Korob, A. Hil, D. Moskovskikh, and V. Romanovski, "Low-Energy Technology for Producing Anhydrite in the CaCO₃ – H₂SO₄ – H₂O System Derived From Industrial Wastes," *Journal of Chemical Technology and Biotechnology* 96, no. 7 (2021): 2065–2071, <https://doi.org/10.1002/jctb.6740>.
45. A. A. Barnabas, O. A. Balogun, A. A. Akinwande, et al., "Reuse of Walnut Shell Waste in the Development of Fired Ceramic Bricks," *Environmental Science and Pollution Research* 30, no. 5 (2023): 11823–11837.
46. A. A. Akinwande, O. A. Balogun, V. Romanovski, H. Danso, M. Kamarou, and A. O. Ademati, "Mechanical Performance and Taguchi Optimization of Kenaf Fiber/Cement-Paperboard Composite for Interior Application," *Environmental Science and Pollution Research* 29 (2022): 52675–52688, <https://doi.org/10.1007/s11356-022-19449-8>.
47. A. O. Ademati, A. A. Akinwande, O. A. Balogun, and V. Romanovski, "Optimization of Bamboo-Fiber-Reinforced Composite-Clay Bricks for Development of Low-Cost Farm-Settlements Towards Boosting Rural Agri-Business in Africa," *Journal of Materials in Civil Engineering* 34 (2022): 1–12, [https://doi.org/10.1061/\(ASCE\)MT.1943-5533.0004489](https://doi.org/10.1061/(ASCE)MT.1943-5533.0004489).
48. A. Adewale Akinwande, D. O. Folorunso, O. A. Balogun, and V. Romanovski, "Mathematical Modelling, Multi-Objective Optimization, and Compliance Reliability of Paper-Derived Eco-Composites," *Environmental Science and Pollution Research* 29, no. 46 (2022): 70135–70157.
49. A. A. Akinwande, D. O. Folorunso, O. A. Balogun, H. Danso, and V. Romanovski, "Paperbricks Produced From Wastes: Modeling and Optimization of Compressive Strength by Response Surface Approach," *Environmental Science and Pollution Research* 30, no. 3 (2023): 8080–8097.
50. A. A. Akinwande, M. S. Kumar, O. S. Adesina, A. A. Adediran, V. Romanovski, and B. Salah, "Tribological Performance of a Novel 7068-Aluminium/Lightweight-High-Entropy-Alloy Fabricated via Powder Metallurgy," *Materials Chemistry and Physics* 308 (2023): 128207.
51. M. Y. Abdulwahid, A. A. Akinwande, M. Kamarou, V. Romanovski, and I. A. Al-Qasem, "The Production of Environmentally Friendly Building Materials out of Recycling Walnut Shell Waste: A Brief Review," *Biomass Conversion and Biorefinery* (2023), <https://doi.org/10.1007/s13399-023-04760-2>.
52. O. S. Adesina, A. A. Akinwande, O. A. Balogun, A. A. Adediran, O. O. Sanyaolu, and V. Romanovski, "Statistical Analysis and Optimization of the Experimental Results on Performance of Green Aluminum-7075 Hybrid Composites," *Journal Of Composites Science* 7, no. 3 (2023): 115.
53. M. S. Kumar, A. A. Akinwande, C. H. Yang, M. Vignesh, and V. Romanovski, "Investigation on Mechanical Behaviour of Al–mg–Si Alloy Hybridized With Calcined Eggshell and TiO₂ Particulates," *Biomass Conversion and Biorefinery* 13 (2023): 1–12.
54. D. C. Combe and E. C. Smith, "Studies on the Preparation of Calcium Sulphate Hemihydrate by an Autoclave Process," *Journal of Applied Chemistry* 10 (1968): 307–312.
55. EN 13279-1:2008, "Gypsum binders and gypsum plasters – Part 1: Definitions and requirements."
56. GOST 23789-2018, "Gypsum binders. Test methods."
57. GOST 1497-84, "Methods of tension test."
58. GOST 4013-2019, "Gypsum and gypsum-anhydrite rock for the manufacture of binders. Specifications."
59. V. Romanovski, X. Su, L. Zhang, et al., "Approaches for Filtrate Utilization From Synthetic Gypsum Production," *Environmental Science and Pollution Research* 30, no. 12 (2023): 33243–33252.
60. EN, B. 13279:2014, *Gypsum Binders and Gypsum Plasters. Definitions and Requirements* (Brussels: European Committee for Standardization, Brussels, 2014) 20 p.
61. M. Kamarou, N. Korob, W. Kwapinski, and V. Romanovski, "High-Quality Gypsum Binders Based on Synthetic Calcium Sulfate Dihydrate Produced From Industrial Waste," *Journal of Industrial and Engineering Chemistry* 100 (2021): 324–332.
62. V. G. Klimenko, "The Role of the Structure and Texture of the Gypsum Matrix in the Formation of Composite Materials," in *Innovations and*

Technologies in Construction: Selected Papers of BUILDINTECH BIT 2020, vol. 95 (Cham: Springer International Publishing, 2021), 233–238.

63. M. Kamarou, M. Kuzmenkov, N. Korob, W. Kwapinski, and V. Romanovski, “Structurally Controlled Synthesis of Calcium Sulphate Dihydrate From Industrial Wastes of Spent Sulphuric Acid and Limestone,” *Environmental Technology & Innovation* 17 (2020): 100582.

64. EN, B. 13279:2014, “Gypsum Binders and Gypsum Plasters.”

Supporting Information

Additional supporting information can be found online in the Supporting Information section.